Soil suction and cracking from the onset to the end of desaturation: micro-scale evidence and model

Tomasz Hueckel, Boleslaw Mielniczuk, Moulay Saïd El Youssoufi, L.B. Hu, Lyesse Laloui

SOIL SUCTION AND CRACKING FROM THE ONSET TO THE END OF DESATURATION: MICRO-SCALE EVIDENCE AND MODEL

T. Hueckel
Department of Civil and Environmental Engineering, Duke University, Durham, NC, USA

B. Mielniczuk and M.S. El Youssoufi
MIST Laboratory, IRSN, CNRS UMR 5508, Montpellier, France

LMGC UMR UM2-CNRS 5508, Université Montpellier 2, 34095 Montpellier Cedex 5, France

L.B. Hu
Department of Civil and Environmental Engineering, University of Toledo, Ohio, USA

L. Laloui
EPFL, Lausanne, Switzerland

ABSTRACT: *A multi-scale, multi-physics sequence of processes is discussed as developing during drying of non-clayey soils. Two variables are believed to be central in drying: suction resulting from the evaporation and effective stress associated with external constraints imposed on drying shrinkage. These two variables are tracked across the scales, both in experiments and simulations. The effective stress is critical as leading eventually to soil drying-cracking. Cracking is a most unwanted development in soil undergoing dewatering. Drying cracks often arise in the apparent absence of external forces. Hence, a tensile eigen-stress pattern resulting from stiff inclusions, or tensile stress produced by reaction forces at the boundary constraints need to be contemplated to reach cracking criteria. An earlier tubular micro-scale model of porous drying medium indicates that transport of water toward evaporating surface during saturation phase induces a high suction. A critical suction value is reached at which water body boundary is penetrated in an unstable manner by air. At the meso-scale such air penetration constitutes a surface imperfection, inducing a total stress concentration near its tip, and in the presence of significant pore suction, a rapid increase in local tensile effective stress and crack propagation. Recent experimental results from a configuration of a cluster of grains provide geometrical data suggesting that an imperfection resulting from of air entry penetrates deep into the granular medium over 4 - 8 radii of the typical pore. Further evolution entails separation of grain clusters by funicular bridge instabilities, and in the last stage formation of two-grain pendular capillary bridges. The final phase is associated with a gradual decrease of the micro-scale suction within these elementary bridges, which eventually evolve into a positive pressure before the bridge rupture.*

1 INTRODUCTION

Suction developing in drying soils and related drying cracking criteria have been intriguing points in unsaturated soil mechanics for some times. The issue starts with often very high values of suction observed from so called soil – water characteristic curves, which taken at face value should generate grain crushing, and culminates with a drying cracking criterion paradox that the tensile drying cracks seem to occur at a compressive effective stress state. The purpose of this paper is to bring together recent micro-scale measurements of capillary forces in model granular systems, numerical simulations of drying at a meso-scale, and provide an approach that disentangles the paradox.

Cracking is almost inevitable in soil structures subject to drying. Desiccation cracking arises in the apparent absence of external forces. Hence, a stress resulting from the reaction

forces generated at the external or internal constraints in response to suction, should be contemplated to arrive at a cracking criterion. Also an internal, self-equilibrated stress pattern due to kinematic incompatibilities, or a non-uniform moisture local content can generate throughtout the drying body (Peron et al., 2009). We apply our recent meso-scale model (Hu et al., 2013a, b, and c) of the shrinkage of drying tubular pores. We hence assess the generated stress in the vicinity of an imperfection, and a stress concentration near its tip, in the presence of significant pore suction. This approach allows us to use the effective stress analysis, which otherwise, away from the stress concentration usually yields compressive effective stress and hence a paradoxical criterion of tensile crack in a compressed body (Scherer, 1990; Hueckel et al., 2011). Experimental results from a hypothetical microstructure of a cluster of grains provide data concerning the evolution of capillary forces during drying and suggesting that events of air entry occur via local pore water surface instability penetrating deep into the granular medium over 4-8 internal radii of the typical pore (Mielniczuk et al., 2013; Hueckel et al., 2013). We postulate that such penetration generates an imperfection in the soil body, to cause a sufficient tensile stress concentration and even in the presence of large suction, the propagation of the drying macro-crack.

2 SCENARIO OF PROCESSES INVOLVED IN DRYING OF POROUS MEDIA

Drying of a porous body is envisioned as a sequence of multi-physics processes that are to be considered at different scales. We start with the observation that the system of pores detected via mercury porosimetry evolves in a particular way during drying (e.g. in Bioley silt, Peron et al., 2009). At different stages of drying, i.e. at the onset at liquid limit, LL, then near shrinkage limit, SL, and at the nearly complete desaturation, D, two classes of pores are seen to evolve in a distinctly different way. These classes, referred to as Large Pores (LP) of around 1.5 μm in diameter and Small Pores (SP) of 0.5 μm do not form any particularly distinct modes originally, but their evolution makes them distinct. As material dries from LL to SL, the Large Pores fraction is reduced to one third and less of the original fraction and altogether disappear at the end of drying (i.e. at w = 0.8%), whereas the volume fraction of the initial SP increases visibly compared to the initial state.

To reproduce this evolution, the medium is idealized as consisting of bunches of parallel cylindrical deformable vessels with two initial diameters, corresponding to LP and SP. There are twelve SPs per one LP in a representative volume, their external wall radius being 3.6 μm, shown in Fig. 1a and b. While we ~~are~~ discuss only 1-D shrinkage, in a more general case the elementary volumes, the pore-vessels can be arranged as in Fig. 1b with 2-D intercalating layers of tubes oriented orthogonally ones to the others. As a result all quantities are appropriately weighed averages of the values pertaining to individual tubes. The vapor flux applied at the pore-vessel end imposes the Poiseuille flow of water throughout the vessel, associated with the shrinkage of tubes, commensurate with the volume of water removed.

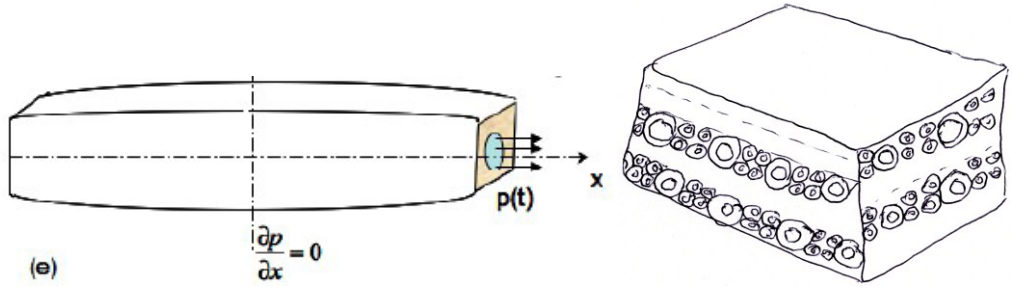

Fig. 1 (a) Model of a deformable pore-vessel subject to evaporation flux; (b) 2-D model of pore-vessels arranged in layers of perpendicular tubes

The water (negative) pressure increases until it reaches a critical value at the vessel exit, at which air penetrates the external boundary of the soil body. Two known criteria, of meniscus plunging and of water cavitation (tensile stress rupture) yield numerically the same criterion. The air entry event starts the second phase of soil desiccation during which the saturation degree actually decreases. In the next phase the evaporating flux is applied at a moving inter-phase interface within the vessel, leading to an increasing presence of the gas phase with the soil body.

The main result from the simulation is the evolution of the (negative) pressure o suction of water. Fig. 2 shows the evolution of pressure in a Large Pore-vessel shortly after it was invaded by air. As seen, the process after the air entry leads to a rapid demise of the pore water pressure, and hence the flow of water. Following the phase of water flow, the next phase consists in an incremental depletion of water via localized phase transition at the moving interface, until all water is gone. In that phase there is no change in pore pressure, hence there is no further volume change of the vessel. Hu et al., 2013b performed simulations of the entire process and the results for the Bioley silt are shown in Fig. 2 in terms of the pore volume change versus water volume loss. Specific instants: of the air entry into LPs, complete cessation of flow in LP, completion of the water removal from all LPs, the air entry into SP, and similar stages in the SP's can be clearly identified. At the meso scale of the assembly of pore-vessels the water pressure is seen to grow only during the flow phase, as a function of the flow dominant pore-vessel diameter, the smallest vessels requiring the highest suctions to activate the flow.

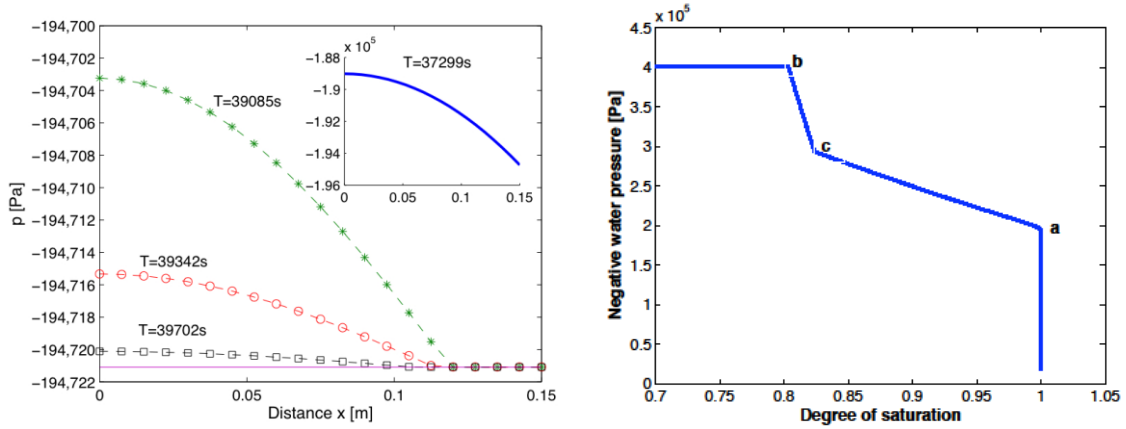

Fig. 2 Evolution of water pressure in pore vessel during drying after air entry into the vessel between *x=0.15* and 0.12 m from the tube center. Shown are three instances 3 minutes one after another, demonstrating a rapid decrease in pressure gradient

Fig. 3 Simulated soil-water characteristic curve obtained via pressure weighing procedure for the systems of the two modes of vessels vs Degree of Saturation

Nevertheless, as seen in Fig. 3, which simulates the soil – water characteristic curve, in this model, the highest suction of the individual smallest pores acts over a decreasing population of pores, and hence does not reach excessively high values per representative volume.

3 AIR ENTRY

The above numerical meso-scale studies calibrated against the experimental results of Peron et al., 2009 yield the value of suction corresponding to the air entry. A numerical criterion for the air entry is generally accepted in soil mechanics (Terzaghi, 1927, see also Lu and Likos, 2003) and expressed via critical pressure difference that of the fluid, p, and atmosphere, p_a, (eq. 1) at a point when a decreasing meniscus radius becomes smaller that the largest pore throat radius. In our case, the radius of meniscus, r, becomes equal to the entrance of the

pore-vessel tube $r = a(t)$, and with τ_s being water surface tension, and θ the wetting angle, the critical pressure reads

$$p - p_a = -\frac{2\tau_s \cos\theta}{r}; r = a|_{x=L} \tag{1}$$

The main point to be stressed is that the change of pore size during drying is substantial, and hence the value of the critical pore size needs to be accordingly adjusted. The resulting values of the critical pore pressure are 194 kPa for the class of large pores of the order of the original 1.5 μm that shrunk to 0.78 μm and 280 kPa for the class of small pores of the order of the original 0.5 μm that shrunk to 0.42 μm (Hu et al., 2013b).

The air entry phenomenon, despite that it occurs at the scale of a single pore, is considered a macroscopic property of soil, mainly based on the assumption of the equality of the fluid pressure at both scales.

A suggestive air entry mechanism in a 2D granular system has been envisioned by Childs (1969) in terms of a succession of stages during drying and re-wetting (Fig. 4).

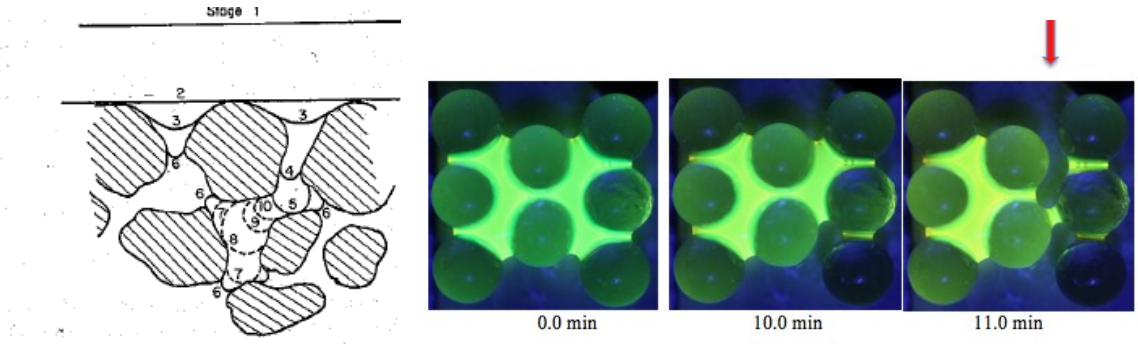

Fig. 4. Succession of meniscus evolution during suction dewatering and rewetting, by Childs (1969)
Fig. 5. Evolution of model grain assembly during drying. The arrow points to air entry sites

However, recent experiments at a meso-scale with drying of model clusters of smooth glass grains (Mielniczuk et al., 2013) with the funicular water bound between them reveal that there are more than a single air entry mode. The most characteristic two modes identified in experimental systems tested of 3, 4, 5, 6 and 8 silica grains in distilled water were two classes corresponding to a negative or positive local Gaussian curvature (which is a product of the two principal curvatures) of the surface of the local meniscus. Most typically, for a negative Gaussian curvature (or concave/convex meniscus) a non-symmetric mode of the unstable evolution of the water body constitutes a most common air entry mechanism into the body of the saturated soil. While the circumstances and numerical criterion for the event are still an open question, it clearly is an unstable and localized displacement of the gas/liquid interface in form of a finger, occurring at a several orders of magnitude higher rate than the preceding process manifested among others by a slow evolution of the liquid/gas interface. Fig. 5 shows three of a series of images of a 2D saturated cluster of 8 grains (Mielniczuk et al., 2013) shot every 90 seconds during natural isothermal drying (using Canon EOS 500D camera). Grains were 3.5 mm in diameter ultrafine silica (glass) spheres, while the liquid is ultra-pure deionized water. As indicated, it took 10 minutes from the initial configuration to reach the intermediate one, and less than 90 additional seconds to develop the final configuration with the gas penetration. The depth of the penetration of the gas finger is about 4 times the average size (diameter) of the pore. For smaller configurations a fast camera

imaging revealed that the unstable process takes about 1/2000-th of a second to develop a new configuration.

An alternative, symmetric entry mode takes place at a point with a positive Gaussian curvature (concave/concave meniscus) between the spheres and consists of a multi- step process: starting with a convergence of two gas/liquid interfaces situated opposite one another (at the front and back of the picture), followed by formation of a suspended thin film of liquid, followed by a further thinning of the film, leading to coalescence of the two surfaces, undergoing what seems like a 2-D water cavitation, which subsequently propagates symmetrically with a circular projection until its boundary reaches the solid walls of the sphere. This is shown in Fig. 6 for a six-sphere cluster. Notably, the non-symmetrical scenario occurs for systems with higher separations between grains, while for lower separations a symmetrical scenario takes place. The unstable part of the process starts at the point when the thin film of water bifurcates. The bifurcations of thin films and thin sheets have been known for sometime (see e.g. Taylor, 1959), but for capillary bridges have been observed only recently by Maeda and Israelachvili (2012) with a mixture of water and vapor molecules, of an intermediate density.

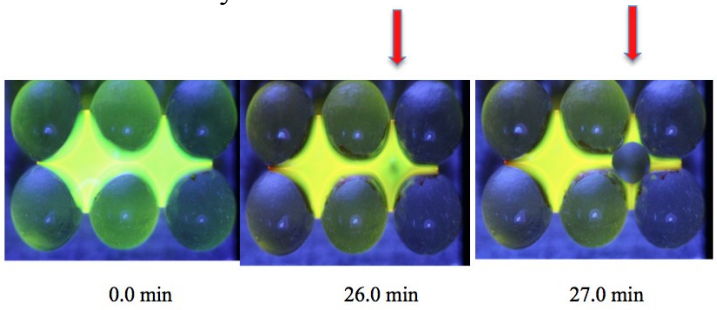

Fig. 6. Evolution of the water body between 6 silica (glass) spheres subjected to evaporation at constant temperature, constant ambient vapor pressure. The red arrow indicates a localized symmetric unstable mode of the interface evolution (air entry via thin film instability)

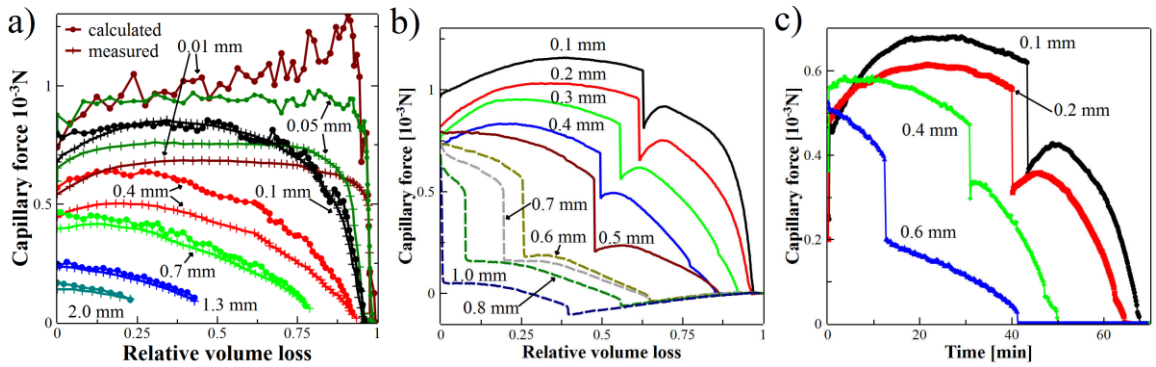

Fig. 7. Evolution of the ~~capillary~~ total resultant capillary force between two spheres during evaporation, calculated from the radii of curvature and measured directly in the experiment (a)~~,~~; measured for 3, (b); and 4 spheres (c).

Interestingly, the symmetric mode of air entry shown above is a prime example of a transformation of a funicular bridge into three pendular ones, which in turn, depending on the inter-granular distance, may undergo a rupture. In general it is seen that the inter-granular force undergoes during evaporation a modest growth above the initial value (up to 20%), to be followed by a steady decline, most commonly to zero. Both events: the air entry and water body rupture, are invariably associated with a substantial discontinuity of the inter-granular force. Fig. 7 shows the evolution of the inter-granular force of systems of 2, 3 and 4 grains

with coplanar positions of their spheres. As seen, the jump of the force reaches up to 70% of the maximum force.

Capillary theory (see e.g. Willett et al., 2000) states that the total inter-granular capillary force, F_C is a sum of two components, resulting respectively from suction in water of capillary bridge acting over the liquid/solid contact and surface tension acting over the perimeter line of solid/liquid/air contact. Both components are proportional to the surface tension coefficient, τ_s, and depend on the radii of curvature of the bridge at the mid height, horizontal, r_g and vertical one, $r_{ext.}$

$$F_C = \tau_s [2\pi r_g + \pi r_g^2 (r_g^{-1} - r_{ext}^{-1})] \qquad (2)$$

The two components for a pendular bridge of 4μm between two silica (glass) grains obtained experimentally for different (constant separations) are shown in Fig. 8. At the beginning of the evaporation, suction force stays more or less steady and the total force is dominated by the surface tension force component. The latter decreases all the time while for smaller separations it accelerates toward the end (last ¼ of the initial water volume) of the process. Notably, at the end of drying both components decrease to zero. It is common in unsaturated soil mechanics to emphasize the role of suction component in suction hardening, while ignoring the surface tension component.

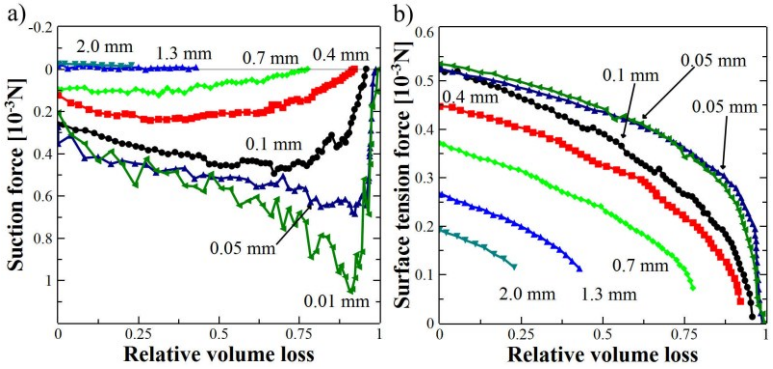

Fig. 8. Evolution of suction force and surface tension force during dryin of two-sphere water bridge

Interestingly, suction in itself, whitch by virtue of Laplace-Young law depends on the sum of the two normal curvatures at the mid height of the pendular bridge, is not neccessarily always positive. For larger separations (> 1mm) it is indeed negative (hence a repulsive pressure, indeed), whereas for the small (including very small) separations it evolves during drying from the initial attractive (suction) to repulsive (pressure) at the small water volumes remaining (Fig. 9). Notably, in a series of parallel experiments of extension of capillary bridges, at various constant values of bridge liquid volume the initial suction transforms into considerable pressure (hence repulsive force).

As seen from Laplace-Young equation (2) this occurs as a direct result of the evolution of the curvatures of the gorge and external (or side) curvature of the neck. The gorge curvature imparts positive pressures, whereas the external curvature induces always suction. The gorge curvature is from the onset larger than the external curvature for 2 and 1.3 mm separations. But for smaller separations, < 0.7 mm, the gorge curvature is initially nearly half or less than the external one, and external curvature is dominant, and practically independent of separation, resulting in a higher suction.

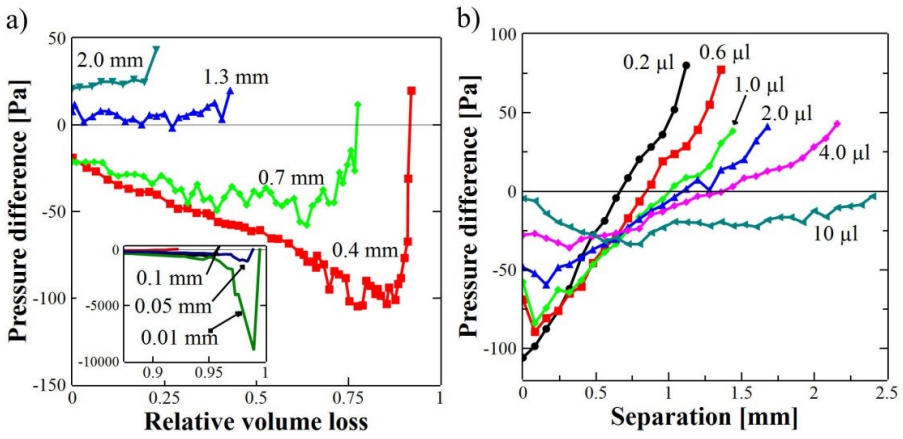

Fig. 9. Evolution of pressure difference (negative means suction) in the capillary bridge between two-grains: (a) during evaporation; (b) during extension

The maximum of suction is the matter of the competing rates of evolution of the two curvatures. Nevertheless, near 90% of water gone, the gorge becomes so tiny, and its curvature very high, resulting hence in a positive pressure. It should be realized that the phenomena described immediately above refer to the very terminal phases of drying of the granular medium. Yet, they indicate quite a complex dynamics of development of suction in capilary bridges, much more than it is usually presented in macro-scopic models of unsaturated soils.

4 DRYING CRACKING

Most of soil systems, either natural or engineered exposed to drying do crack at some point, unless drying occurs in idealized conditions of no kinematic constraints whatsoever. The occurrence of cracking, which takes place at a surprisingly narrow range of water content, changes substantially both the dynamics of further evaporation and the configuration, and hence the mechanical boundary conditions of the unsaturated soils. Those two aspects are widely ignored in the unsaturated soil mechanics.

As mentioned earlier, criteria of desiccation cracking via macroscopic approach suffer from a major handicap. A consideration of a 1D drying of a constrained saturated granular body easily shows that a modest total stress is generated in reaction to the constraints and that it is tensile, whereas the values of suction induced by the evaporation flux is significant. Consequently, the resulting effective stress appears to be compressive. This is counterintuitive, as drying failure evidently occurs through tensile cracking.

Scherer (1992) postulated a scenario, suggesting that desiccation cracking is necessarily triggered through crack propagation from a tip of a pre-existing structural flaw in the soil body, at which a substantial total stress concentration occurs. Consequently, the remote total stress is augmented locally through a stress concentration and becomes larger in absolute terms than the elevated suction. As a result the local effective stress becomes tensile, and hence prone to reach the tensile strength of the material, and thus prompting the crack propagation evolving from the material flaw.

We postulate that a non-symmetric finger of air entry as described above, constitutes a sufficient imperfection (flaw) in the drying granular body to produce enough of a concentration of total stress induced by the kinematic restraints to the drying shrinkage around the tip of the flaw, to generate crack propagation, as proposed by Péron et al., 2010, and Hu et al., 2011.

Within the above framework we consider an air finger (flaw) with depth c and curvature radius at the finger tip of r_c at the soil surface, which is surrounded by the micro-tubes pore system as shown in Fig.10. The network of hollow cylinder pore-vessels of micro-tubes representing at the meso-scale the pore system is adapted from the model of Hu et al., 2013a to simulate the shrinkage mechanism for silty soil due to water evaporation. The external radius (R_{ext}) of the tubes equal to $3.6\mu m$ is calculated from the measured macroscopic porosity and the initial and current internal radius (R_{int}) are equal to 1.5 and 0.75 μm, respectively. These radii are identified as representative of Large Pores based on the mercury intrusion porosimetry data on Bioley silt and calibrated simulation (Hu et al., 2013 a, b). Using the principles of linear fracture mechanics, the stress at the external boundary of the tubes, which are placed near the flaw tip can be calculated as the far-field (macro-scale) stress at crack initiation as (stress is positive in tension)

$$\sigma_x = \frac{K_{I\,crit} + \frac{1}{2} p\sqrt{\pi r_c}}{B\sqrt{\pi c}} \tag{3}$$

where $K_{I\,crit}$ is the critical stress intensity factor, B is a constant equal to 1.12 and p is the fluid pressure inside of the pore (Scherer, 1992).

The depth of a flaw (c) can be estimated from Fig. 4b as 2-4 times the diameter of the original biggest pore, assessed for Bioley silt as d=1.5 μm (hence c =7.5 μm for that silt). Hu et al., 2013a. The flaw tip curvature radius r_c is found to be of the same order as the internal radius of the biggest pore (d/2=0.375 μm). A desiccation crack is generally initiated when the soil suction reaches the suction value at the air entry moment. Considering the biggest current pore size of $0.75\mu m$, the suction value at air entry for Bioley silt has been calculated as 194 kPa (Hu et al., 2013b). Adopting a value of 0.16 kN/m$^{3/2}$ for the critical stress intensity factor as measured by Chertkov (1995) for a sandy silt soil, a value of σ_x = 39kPa is obtained for the macro scale total stress from Eq. 3. This value is close enough to the one obtained experimentally by Péron (2008) in simulations of the drying experiments on constrained slabs of Bioley silt (25 kPa). The local total stress at the flaw tip is hence estimated as

$$\sigma_c^{\max} = 2B\sigma_x\sqrt{\frac{c}{r_c}} \tag{4}$$

which yields a value of 295 kPa (tension), which translates into about 101 kPa of the local effective tensile stress at the crack tip. That is equivalent to compressive 235 kPa of effective macro-scale stress at cracking.

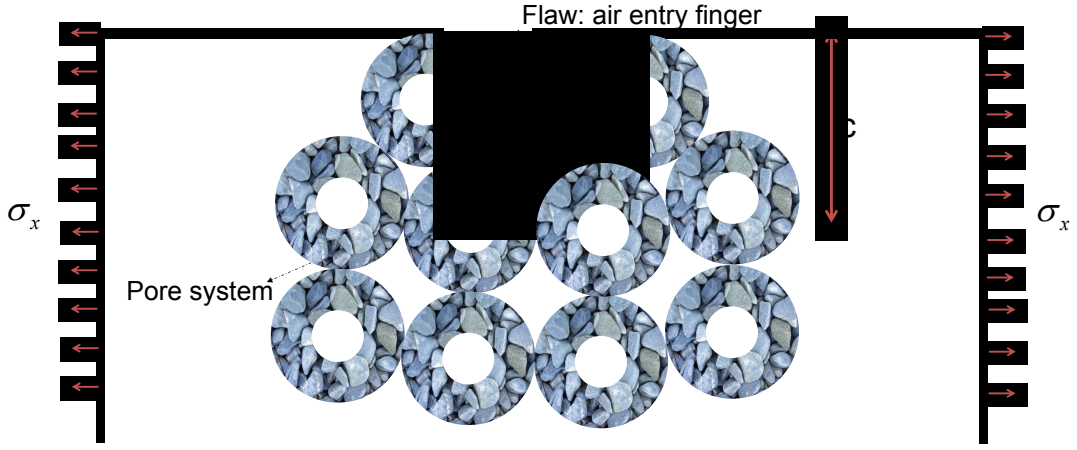

Fig. 10. An idealized meso-scale pore network in the vicinity of an air finger

5. CONCLUSIONS

A multi-scale scenario of evolution of suction, effective stress, air entry and cracking during drying of non-clayey soils is discussed in view of macro-, meso- and micro- scale experiments. While the picture emerging is far from being complete, some findings are consistent with, and some different, from the current thinking in unsaturated soil mechanics. The evolution of resultant inter-granular forces during drying needs to be considered, rather than that of suction alone. Indeed, the effect of surface tension during drying may become dominant in inter-granular interactions toward end of drying. Suction per se undergoes evolution from positive to negative, hence exerting repulsion across the liquid bridge. In no investigated case any dramatic increase of suction toward the end of drying was seen.

The air entry was observed on granular models as an unstable evolution of the liquid body surface in a variety of forms. One of the forms is penetration of an air pocket with depth of 3-8 radii of the typical largest pore. The penetration is seen to be associated with a sudden decrease by half of inter-granular force. No particular condition for the instability producing the air entry has been identified, as yet.

The air entry has been postulated to for a material imperfection, giving rise to the total stress concentration near its tip. The stress arises in response to constraining drying shrinkage at the substrate or reaction points. Such stress concentration, is shown in a linear elasticity fracture mechanics parametric study to produce a sufficiently high hike in the local tensile effective stress value to promote the growth of tensile crack, despite high suction and hence a compressive effective stress at a macro-scale. As the air entry constitutes a common and ubiquitous occurrence, and most of drying bodies are constrained in their shrinkage, the above postulate appears to yield a reasonable criterion for drying cracking.

ACKNOWLEDGEMENT

Portion of the work has been funded by the US NSF, grant No. 0324543 of CMMI Division, Geomechanics and Geomaterials Program (T. Hueckel) and support of CNRS, MIST laboratory and the Languedoc-Roussillon region (B. Mielniczuk, M. S. El Youssoufi, T. Hueckel).

.

REFERENCES

Childs E.C. (*1969*) An introduction to the physical basis of *soil* water phenomena. London: Wiley, Interscience.

Chertkov, V.Y., (1995), Evaluation for soil of crack net connectedness and critical stress intensity factor, Int. Agrophysics, 9, 189 -195

Hu, L.B. H. Peron, L. Laloui and T. Hueckel, A multi-scale multi-physics model of soil drying, Geofrontiers, 2011,

Hu, L. B., H. Péron, T. Hueckel, L. Laloui, (2013a) Desiccation shrinkage of non-clayey soils: multi-physics mechanisms and a microstructural model, Int. J. Numer. Anal. Meth. Geomech, DOI: 10.1002/nag.2108.

Hu, L. B., H. Péron, T. Hueckel, L. Laloui, (2013b) Desiccation shrinkage of non-clayey soils: a numerical study, Int. J. Numer. Anal. Meth. Geomech., DOI: 10.1002/nag.2107

Hu, L. B., H. Péron, T. Hueckel, L. Laloui, (2013c) Mechanisms and critical properties in drying shrinkage of soils: experimental and numerical parametric studies, Can. G. J., in

print
Hu, L. B., M. Monfared, B. Mielniczuk, L. Laloui, T. Hueckel, M. S. El Youssoufi, 2013, Multi-scale approach to cracking criteria for drying soils, GeoCongress, ASCE 2013, 838 -845
Kodikara J., Barbour S.L., Fredlund D.G., 1999, Changes in clay structure and behaviour due to wetting and drying. in Proceedings of the eighth Australia-New Zealand Conference on Geomechanics, Vitharana ND, Colman R (eds). Hobart, Australia, 1999; 179–185.
Lu, N. and Likos, W., 2003,
Maeda, N; Israelashvili, JN; Kohonen, MM, 2003, Evaporation and instabilities of microscopic capillary bridges, Proc. National Academy of Sciences: 100, 3: 803-808
Mielniczuk, B., T. Hueckel, M. S. El Youssoufi (2013) Micro-scale study of rupture in desiccating granular media, GEO-CONGRESS 2013,
Pellenq RJM, Coasne B, Denoyel RO, Coussy O. 2009, Simple phenomenological model for phase transitions in confined geometry. 2. Capillary condensation/evaporation in cylindrical mesopores. Langmuir 25(3):1393–1402.
Péron, H.,T. Hueckel, L. Laloui, L.B. Hu (2009), Fundamentals of desiccation cracking of fine-grained soils: experimental characterization and mechanism identification, Canadian Geotechnical J., 46, 1177-1201
Péron, H., L. Laloui, L.B. Hu, and T. Hueckel (2010), Desiccation of drying soils, in Mechanics of Unsaturated Geomaterials, p. 55-86, edited by L. Laloui, J. Wiley, Hoboken, NJ,
Péron, H. (2008) Desiccation cracking of soils, PhD thesis, EPFL, Lausanne
Scherer G.W., 1992, Crack-tip stress in gels, *J. Non-Cryst. Solids*, vol. 144, 210-216
Taylor, G.I., 1959, The dynamics of thin sheets of fluid. III. Disintegration of fluid sheets, Proc. R. Soc. London, Ser. A 253, 313 ~1959
Terzaghi K., 1927, Concrete roads - A problem in foundation engineering. Journal of the Boston Society of Civil Engineers 1927; 14:265–282.
Willett, Ch. D., Adams, M. J., Johnson, S. A., Seville, J. P. K. (2000). Capillary bridges between two spherical bodies, *Langmuir* 16: 93-96.